Tetrahedron Vol. 46, No. 8, pp. 2747-2760, 1990
Printed in Great Britain

0040-4020/90 $3.00+.00

ISOLATION AND CHARACTERIZATION OF A PRESUMED BIOSYNTHETIC PRECURSOR OF CAMPTOTHECIN FROM EXTRACTS OF *CAMPTOTHECA ACUMINATA*

Brad K. Carte',[a] Charles DeBrosse,[b] Drake Eggleston,[c] Mark Hemling,[c] Mary Mentzer,[c]
Benjamin Poehland,[a] Nelson Troupe[a] and John W. Westley[a]*

Departments of Biomolecular Discovery,[a] Analytical[b] and Physical & Structural Chemistry[c]
SmithKline Beecham Pharmaceuticals, Research and Development
P.O. Box 1539, King of Prussia, PA 19406-0939

Sidney M. Hecht
Departments of Chemistry and Biology, University of Virginia, Charlottesville, Virginia 22901

(*Received in USA* 21 *December* 1989)

Abstract. A biosynthetic precursor **4** of the antitumor alkaloid camptothecin (**1**) has been isolated from alkaloid enriched extracts of *Camptotheca acuminata*. The structure of **4**, which was determined both in the solid state by x-ray diffraction and in solution by NMR analysis, provides strong evidence in support of the proposed biosynthetic scheme for camptothecin (**1**).

The isolation of the novel pyrrolo[3,4-b]quinoline alkaloid camptothecin (**1**) from *Camptotheca acuminata* Decne (Nyssaceae) was first reported in 1966[1] as part of an antitumor screening program carried out under the auspices of the National Cancer Institute of the National Institutes of Health. The structure of **1** was deduced from its spectral properties and the x-ray crystallographic analysis of its 20-iodoacetate derivative[2] which established the structure as 4(S)-4-ethyl-4-hydroxy-1H-pyrano[3',4':6,7]indolizino[1,2-b]quinoline-3,14[4H,12H]-dione. Camptothecin has also been isolated from *Nothapodytes foetida* (Wight) Sleumer (Icacinaceae),[3] *Ophiorrhiza mungos* Linn. (Rubiacea)[4] and *Ervatmia heyneana* (Wall) T. Cooke (Apocynaceae).[5] The chemistry and biosynthesis of camptothecin have been reviewed by Hutchinson.[6] Interest in camptothecin has been renewed since the discovery that the alkaloid induces site-specific single strand cleavage of DNA in the presence of topoisomerase I[7] and that the compound's cytotoxic activity has been correlated with its effect on topoisomerase I in mammalian cells.[8-10]

In addition to camptothecin (**1**), a number of oxygenated analogues including the 9-methoxy (**2a**), 10-hydroxy (**2b**),[11-12] 10-methoxy (**2c**),[13] 11-hydroxy (**2d**)[14] and the 18-hydroxy (**2e**)[15] derivatives also have been isolated from these plants. In order to obtain gram quantities of both camptothecin (**1**) and any of the oxygenated analogues (**2a-e**) for the semisynthetic preparation of water soluble camptothecin derivatives,[16] the polar fraction of a large scale extract of *Camptotheca acuminata* was subjected to a detailed study as described in this paper. As a result, in addition to **1**, **2b** and **2e** we also isolated the pyridino-indolo-quinolizidinone alkaloid angustoline (**3**), previously known from *Strychnos angustiflora*,[17] and a glycoside, [3S-(3α,4β, 4aα, 5aβ)]-4-ethenyl-3-(β-D-glucopyranosyloxy)-4,4a,5,5a,6,12-hexahydro-3H-pyrano[3',4':6,7] indolizino [1,2-b]quinoline-11,14-dione, **4**. During preparation of this manuscript, the isolation of **4** from *Ophiorrhiza pumila* (Rubiaceae) was reported.[18]

The starting material for this study was a sample (FB-12100B) from the isopropanol/0.25% ammonia eluate from ion-exchange (Amberlyst 15) chromatography of the IPA extract of *C. acuminata*. Sample FB-12100B was partitioned between water and ethyl acetate and the aqueous layer was extracted further with n-butanol. Silica gel chromatography of the EtOAc layer gave camptothecin (**1**), 10-hydroxycamptothecin (**2b**), 18-hydroxy-

camptothecin (**2e**) and angustoline (**3**) which were identified by comparison with authentic standards (**1 and 2b**) or by comparison of spectral data with published values (**2e and 3**). Sephadex LH-20 chromatography of the 1:1 $MeOH/CH_2Cl_2$ soluble portion of the butanol layer gave glycoside **4** which crystallized from $MeOH/H_2O$ as colorless plates (mp 288-290°C). Progress in the purification of all compounds was monitored using an analytical reversed-phase HPLC assay described elsewhere.[19]

High resolution FAB mass spectrometry established the molecular formula of **4** as $C_{26}H_{28}N_2O_9$ which differs from camptothecin (**1**) by a $C_6H_{12}O_5$ unit indicating that **4** was possibly a hexosyl-camptothecin derivative with one additional site of saturation. This was supported by the strong fragment ion at m/z 351 (M+H - 162) and by methanolysis of **4** to give the aglycone (**6**) and D-glucose.

Examination of the ^1H, ^1H COSY, ^{13}C and $^1H/^{13}C$ correlation NMR spectra of **4** revealed several prominent features. Clearly evident were proton signals arising from a 1,2-disubstituted aromatic ring similar to that found in camptothecin (**1**). Also evident was the lack of signals corresponding to the terminal C18-C19 ethyl group in camptothecin. The ^1H NMR spectrum of **4**, however, exhibited signals suggesting a terminal vinyl group attached to a methine carbon, based on analysis of coupling patterns and the presence of a triplet ^{13}C signal in the aromatic region of the spectrum (δ120.5). This provided a convenient starting point for the analysis of the ^1H COSY spectrum which permitted determination of substructure **5**.

The $^1H/^{13}C$ correlation spectrum showed the carbon (t, δ120.5) to be attached to two protons, at δ5.33 and 5.47, which were observed in the COSY spectrum to be coupled to an olefinic methine (δ5.79). This methine, in turn, was observed to be coupled to an allylic methine proton (δ2.63). This methine showed couplings to another methine proton (δ3.26) and to a downfield proton, δ5.38, whose associated ^{13}C shift, δ94.9, suggested an acetal center. This proton showed no further couplings and must represent one end of the coupling network.

The methine proton at δ3.26 showed coupling in the COSY spectrum to a proton at δ2.01, which is one of a pair of geminally coupled methylene signals (δ2.01, 2.47). The geminal nature of these protons was confirmed by their mutual correlation to a ^{13}C triplet, δ28.1. These protons were both coupled to a methine proton at δ4.75. This methine proton showed small couplings to each of a pair of methylene protons (δ4.47, 4.32; ^{13}C, t, δ47.4), which is the other terminus of the network of coupled spins. The small J values shown by both of these methylene signals to δ4.75 suggested that these protons were removed by more than three bonds from the methine and that the coupling was long-range. The ^{13}C shifts of this methylene carbon and that of the carbon attached to the δ4.47 methine (δ59.4) suggested that each was bonded to nitrogen; on the assumption that only two nitrogen atoms were present and one of these was associated with the quinoline, this further suggested that they were coupled to the same nitrogen. This would accommodate the long-range coupling and permitted assembly of partial structure **5**.

The methine at δ3.26 also showed a long-range coupling to a proton whose downfield shift (δ7.04, d, J=2.7 Hz) and associated ^{13}C shift, δ145.1 suggested an enol ether. This assignment was supported by the presence of a ^{13}C singlet at δ108.9. The β carbon in this enol ether fragment must therefore occupy a ring junction.

The observation of a hexosyl fragment in the mass spectrum of **4** was fully supported by observation in the proton and ^{13}C NMR spectra of a subset of spectral lines similar in intensity to those of the camptothecin nucleus and whose proton shifts were correlated in the COSY experiment. The ^{13}C doublet at δ97.8 was directly

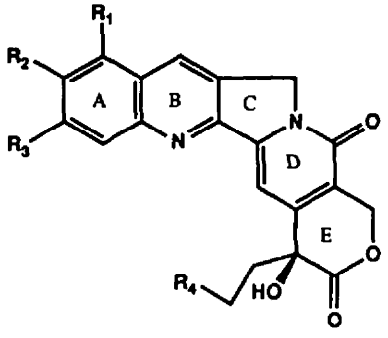

1: $R_1=R_2=R_3=R_4=H$
2a: $R_1=OMe$, $R_2=R_3=R_4=H$
2b: $R_1=R_3=R_4=H$, $R_2=OH$
2c: $R_1=R_3=R_4=H$, $R_2=OMe$
2d: $R_1=R_2=R_4=H$, $R_3=OH$
2e: $R_1=R_2=R_3=H$, $R_4=OH$

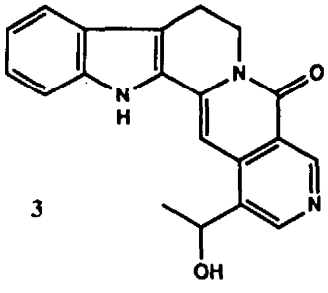

3

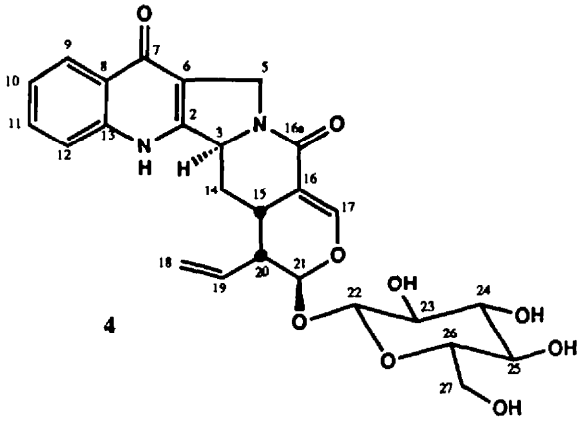

4

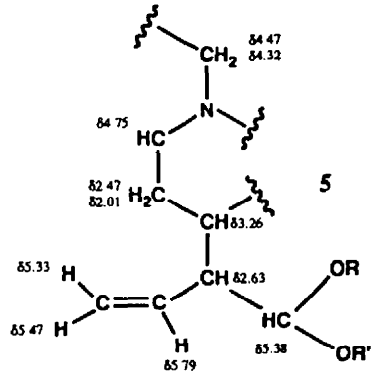

5

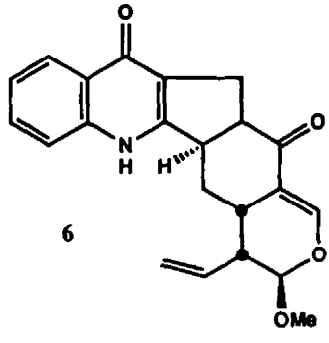

6

coupled to a proton doublet, δ4.54, suggesting an anomeric methine, which in turn was observed to couple (J=7.8) into a set of sugar methine protons in the region δ3.0-3.3. This network terminated in a pair of methylene protons at δ3.69 and δ3.43. The vicinal coupling constants among the methine protons were each ca. 9.5 Hz as determined through selective decoupling experiments following deuterium exchange. These couplings implied that the sugar fragment was glucose. Five hydroxyl protons were observed to be coupled to individual glucose protons in the COSY spectrum and were exchanged upon D_2O addition.

The stereochemistry of the attachment of glucose to the camptothecin nucleus was revealed by the direct $^1J_{CH}$ for the anomeric carbon, determined in a fully coupled ^{13}C NMR spectrum to be 161.2 Hz.[20] This strongly suggested that the anomeric proton was axial. While the 7.8 Hz coupling between the anomeric proton and its vicinal partner was somewhat smaller than usually observed for trans-diaxial protons, it clearly excluded an axial–equatorial relationship. Therefore the linkage between the glucosyl moiety and the camptothecin nucleus was assigned as β.

The presence of the acetal carbon in the camptothecin spectrum taken together with that of the glucosyl moiety suggest that the acetal was stabilized by glycosylation. Other salient features of the ^{13}C NMR spectrum include two carbonyl signals, and four other quaternary carbons, as expected for the quinoline moiety in the camptothecinoid nucleus. The NMR data, in conjunction with mass spectral analysis, permitted determination of structure **4**. The tautomeric nature of the 4-pyridone ring was demonstrated by X-ray diffraction analysis as discussed below. The keto form as described would better accommodate the chemical shift of the exchangeable (NH) proton, δ12.1, than would a 4-hydroxypyridine structure. Given the keto-tautomer, it becomes possible to rationalize the chemical shift assignments for the aromatic quaternary ^{13}C signals based, for example, on those for ribalinine and isoplatydesmine.[21] Attempts to assign the quaternary ^{13}C using COLOC experiments were unsuccessful. This tautomer requires reversal of the usual chemical shift order for aromatic protons 9 and 12, consistent with the proximity of H9 to the carbonyl at C7.

Apparent first-order coupling constants were extracted from resolution-enhanced 1-D ^1H NMR spectra of **4** in DMSO-d6. Table 1 gives the chemical shift assignments and couplings observed for **4**. The large number of splittings present on H15 and H3 required indirect assessment of those couplings from examining the patterns on other protons known from the COSY experiment to be coupled to them. The couplings thus extracted were used to simulate the patterns observed for H15 and H3, which are indicated in parentheses in Table 1. A large coupling (J=12.2 Hz) was clearly present on H3. The COSY experiment failed to show a cross-peak relating H14(1) to H-15 either prior to or following deuterium exchange, presumably due to the small coupling constant (<1 Hz) and diffuse patterns for both protons.

Cursory analysis of the coupling constant data for the spin network defined by CH3–$CH_2$14(1,2)–CH15–CH20–CH21 would have suggested a stereochemical arrangement in which both H3 and H15 were approximately trans-diaxial with respect to H14(2)(δ2.01), exhibiting coupling constants of 12.3 and 9.9, respectively. H20 would then be cis to H15 and trans to H21, with both H20 and H21 occupying equatorial positions on ring E. MM2 minimization of such a structure produced a model in which rings D and E adopt flattened-chair conformations, in reasonable agreement with the observed coupling constant values.

X-ray diffraction analysis of **4**, however, demonstrated that the stereochemical relationship between H3 and H15 is trans, with H20 cis to H15 and trans to H21. Such an arrangement necessarily excludes the mutually trans relationship of H3 and H15 with H14(2) as suggested above. The corrected stereochemical assignments

were therefore used in construction of models for **6**, using MACROMODEL©. These were subjected to iterative MM2 minimization. By deliberate distortion of selected bond angles and interatomic distances before minimization, at least four reasonably distinct conformational minima were determined for **6**.

Table 1. ^1H (360 MHz) and ^{13}C (90.56 MHz) NMR Data for Glycoside **4**, in DMSO-d_6.

Atom#	δH (intensity, multiplicity, J(Hz))	δC (multiplicity)†
1(NH)	12.10 (1H, s)	--
2	--	149.7 (s)
3	4.75 (1H, dxm, J=12.2, complex (12.2, 2.7, 1.5 3.8)	59.4 (d)
5(1)	4.47 (1H, dxd, J=14.3, 2.6)	47.4 (t)
5(2)	4.32 (1H, dxd, J=14.3, <1)	"
6	--	112.9 (s)
7	--	173.0 (s)
8	--	125.3 (s)
9	8.12 (1H, dxd, J=8.1,1.4)	124.7 (d)
10	7.33 (1H, dxdxd, J=1.1, 8.1, 8.4)	123.2 (d)
11	7.65 (1H, dxdxd, J=8.4, 8.1, 1.6)	131.6 (d)
12	7.58 (1H, dxd, J=8.1, ca.1)	118.3 (d)
13	--	140.4 (s)
14(1)	2.47 (1H, dxdxd, J=13.2, 3.6, ca. 0.9)	28.1 (t)
14(2)	2.01 (1H, dxdxd, J=13.2, 12.3, 9.9)	"
15	3.26 (1H, complex mult.) (J=9.9, 4.8, 0.9, 2.7)	23.7 (d)
16	--	108.9 (s)
16a	--	163.9 (s)
17	7.04 (1H, d, J=2.7)	145.1 (d)
18(trans)	5.47 (1H, dxd, J=17.1, 2.1)	120.5 (t)
18(cis)	5.33 (1H, dxd, J=10.3, 2.1)	"
19	5.79 (1H, dxdxd, J=17.1, 10.3, 9.1)	132.5 (d)
20	2.64 (1H, dxdxd, J=9.1, 4.8, ca. 1.5)	43.6 (d)
21	5.38 (1H, d, J=1.6)	94.9 (d)
22	4.54 (1H, d, J=7.8)	97.8 (d)
23	2.97 (1H, complex multiplet*)	73.2 (d)
24(overlapped with H26)	3.16 (1H, complex multiplet*)	77.3 (76.5) (d)
25	3.03 (1H, complex multiplet*)	70.1 (d)
26(overlapped with H24)	3.16 (1H, complex multiplet*)	76.5 (77.3) (d)
27(1)	3.69 (1H, 6.4,12.2, ca 1)	61.1 (t)
27(2)	3.43 (1H, 6.1, 12.2, 6.1)	"
23-25,27(OH)	4.99,4.98,4.92,4.56 (4H, d)‡	--

*each of these signals gave a dxd, J=J=ca. 9.5, on D_2O exchange.
†The multiplicities of ^{13}C were determined through a combination of GASPE (GAted-SPin-Echo) and $^{13}C/^1H$ correlation experiments.
‡These signals were exchanged on addition of D_2O, and are not individually assigned.

One of the minimized structures for **6**, shown below, showed dihedral angles among the protons in the critical spin network that permitted close agreement between the calculated and observed values for the coupling constants for **4**. This conformation is characterized by a twist-boat conformation for the D ring, with a dihedral relationship between C3 and C20 of -107°. The large value for $^3J_{14(2)-15}$ observed (ca. 9.9 Hz) is consistent with the small dihedral angle subtended by those protons, 17.9°. The H20–H21 coupling constant is consistent with a distorted chair conformation for the E ring, such that the 20-vinyl and 21-alkoxy substituents are trans-diaxial and

both C20 and C3 lie to the same side of a plane described by C14,C15,N4 and C16a. The vicinal coupling constants calculated based on this model are compared with the observed values for **4** in Table 2.

Table 2. Calculated vicinal coupling constants for the modeled structure, compared with experimental values for **4**.

Protons	^{3}J(calc'd.*) Hz	^{3}J(observed) Hz
H3—H14(2)	11.8	12.3
H3—H14(1)	3.4	3.8
H14(2)—H15	9.4	9.9
H14(1)—H15	1.5	ca. 1
H15—H20	3.0	4.8
H20—21	1.8	1.6

*Calculated using MACROMODEL® according to Altona.[22]

Although only the relative configurations for carbons 3,15,20 and 21 obtained from X-ray diffraction of **4** were used in the modeling process, the model that finally allowed correct prediction of the coupling constants matched closely the torsional angles for the camptothecinoid nucleus determined in the diffraction analysis.

Both protons on C5 exhibited long-range couplings with H3. The model described above does not predict a "planar W" pathway connecting either of these pairs, although both bear homoallylic relationships that would be predicted to show significant couplings according to $^5J = K(\sin^2\phi\sin^2\phi')$ where ϕ and ϕ' are the dihedral angles subtended between each homoallylic proton and the carbons in the double bond.[23] The slightly smaller angle predicted for H5(1) (112.6°) compared with H5(2) (119.9°) suggested that the proton at δ4.47 (^5J=2.6 Hz) was H5(1), although given that homoallylic coupling in five-membered rings is complicated by the presence of a four-bond path, it cannot be reliably used for the assignment.

The structure closely matching that determined by X-ray diffraction analysis for the camptothecin moiety is given below. The subtleties required in interpretation of the coupling patterns and the initially erroneous assignment of the stereochemistry underscore the need for cautious interpretation of J values, given that two possible dihedral angles can be obtained from a specific J value, and the potential for perturbations on the Karplus relation by the presence of heteroatoms.

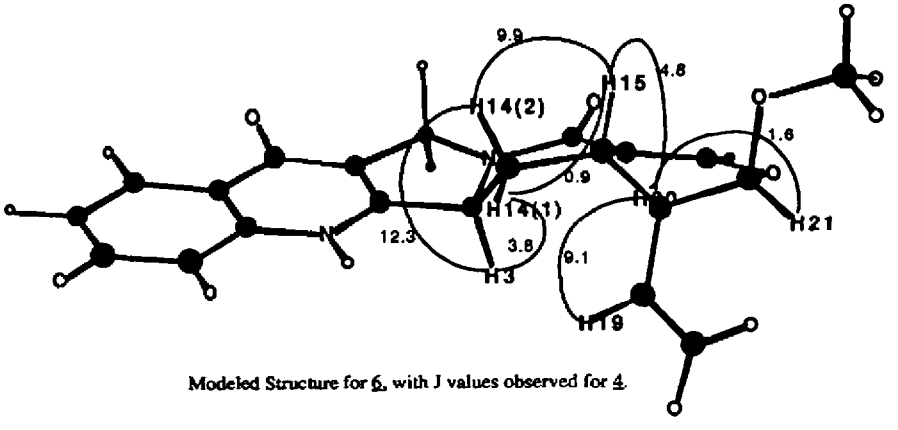

Modeled Structure for 6, with J values observed for 4.

The structure of **4** is of particular interest because the compound appears to be a biosynthetic precursor of camptothecin (**1**). The biosynthesis of camptothecin has been the subject of considerable speculation, experimentation and review.[6] One year after the structure of camptothecin was published,[1] Wenkert[24] proposed that the compound was derived biosynthetically from a monoterpene indole alkaloid precursor and Winterfeldt[25] elaborated on this proposal based on his observation that indole alkaloids undergo facile autoxidation to the pyrrole[3,4-b]quinoline chromophore present in **1**. In fact an intermediate in the oxidative transformation of the indole to quinole ring system is the 4-quinolone chromophore present in the glycoside **4**. Hutchinson *et al*[26] recognized the structural relationship between **1** and strictosamide (**7**). Strictosamide is known to be a basic transformation product of strictosidine,[27] or isovincoside (**8**) which in turn is derived from tryptamine (**9**) and secologanin (**10**) via a formal Pictet-Spengler condensation[28] as illustrated in Figure 2. Completion of the biosynthesis of camptothecin from **7** was considered by Hutchinson,[6] and independently by Cordell[29] to be accomplished by the aforementioned autoxidation-recyclization of rings B and C, ring D oxidation, removal of the C-21 glucose and finally ring E oxidation. Corroboration of the site-specific incorporation of **7** into **1** has been established[26] using ^{13}C-labelled precursor and our isolation and characterization of **4** provides further strong evidence in support of the biosynthetic scheme as illustrated. In particular, the S-configuration at the C-3 position in compound **4** confirms the intermediacy of isovincoside (**8**) rather than its C-3 epimer, vincoside, in the biosynthesis of camptothecin.

In his proposal of post-strictosamide (**7**) biosynthesis of camptothecin, Hutchinson[6] suggested that the removal of glucose from **7** probably would be the next step towards the formation of the camptothecin skeleton, but with the discovery of **4**, this is now clearly not the case. The next step must involve the oxidation-recyclization of **7**, in which the indole chromophore is converted by oxidation of the 2,3-double bond to an intermediate, equivalent to compound **11**, which then cyclizes to the pyrrolo[3-4-b]quinolone present in glycoside **4**. This reaction, first proposed by Wenkert[24] and Winterfeldt,[25] is based on a reaction well documented in the literature and know to proceed via periodate,[30] peroxide[31] or aerial oxidation.[32] A possible next step in the biosynthesis of camptothecin is suggested in Figure 1 as an isomerization of the enol ether double bond in **4** to the endocyclic double bond proposed in **12**.

X-RAY CRYSTALLOGRAPHY

The structure of **4** was confirmed by a single crystal x-ray diffraction study; an ORTEP[33] diagram of the molecular structure is presented in Figure 2. Assuming, as shown, that the glucose moiety has the D configuration the assignments at other asymmetric centers are S at C-3, S at C-15, S at C-20 and R at C-21. The relative stereochemistry observed for C-3 and C-15 agrees with that determined for the related indole alkaloid hunterburnine.[34] The glucose is β-linked to the camptothecinoid ring system, in agreement with the NMR studies showing an axial anomeric proton.

Crystal Data. $C_{26}H_{28}N_2O_9 \cdot 3H_2O$, M = 566.57, orthorhombic, $P2_12_12_1$, a=7.984(3), b=8.995(4), c=36.241(13)A, V=2602.8A^3, D_c(Z=4)=1.446gcm^{-3}, F(000)=1200, μ=1.077 cm^{-1} for graphite monochromatized MoKα radiation (λ=0.71073A), specimen: 0.15 x 0.25 x 0.26 mm colorless plate from aqueous methanol, T=295K.

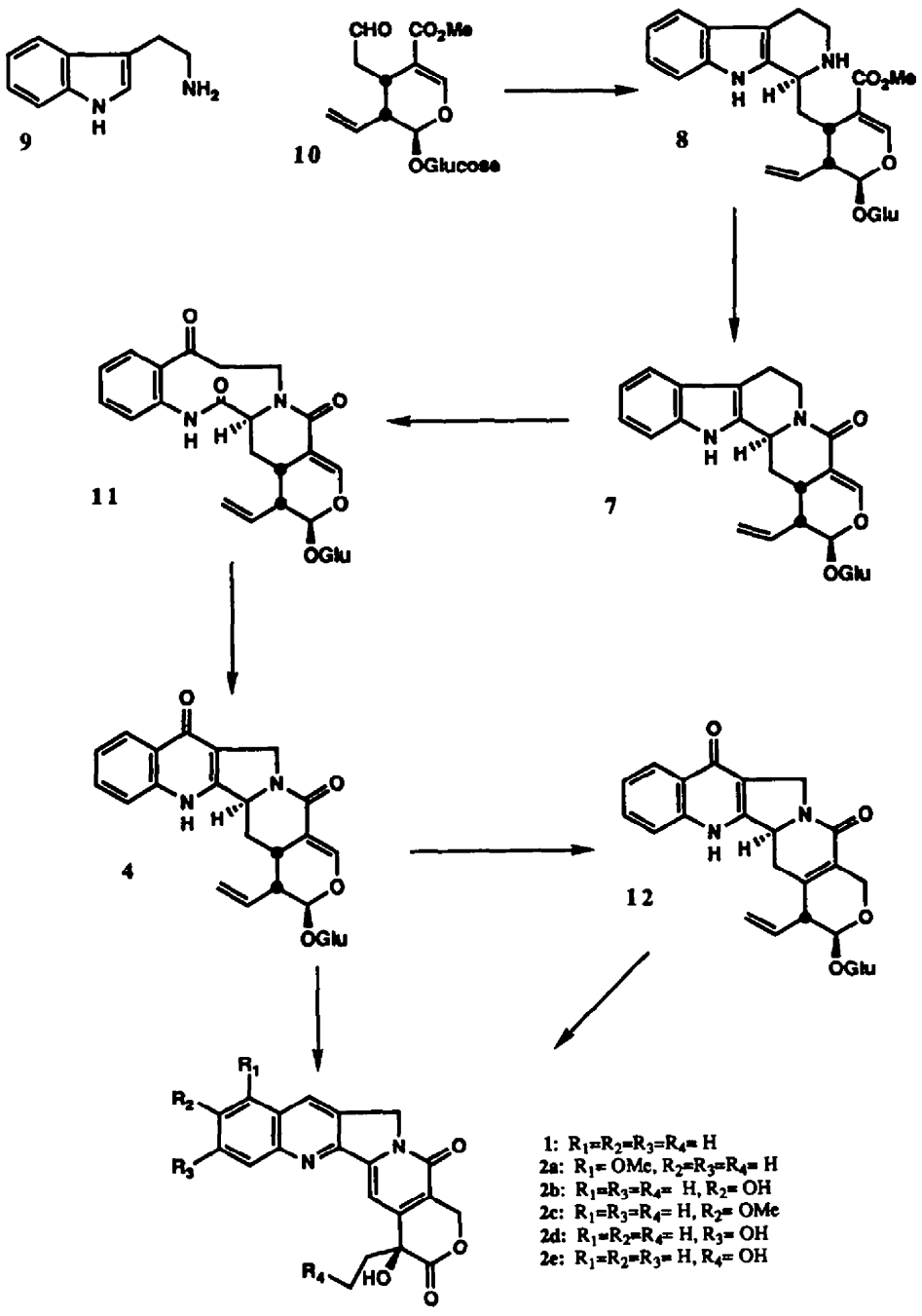

Figure 1. Hypothetical scheme for the biosynthesis of camptothecin (1) and metabolites (2) via the intermediate 4.

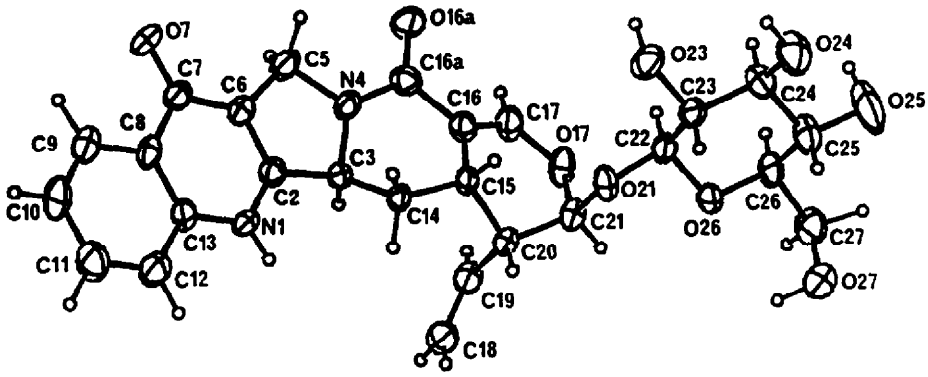

Figure 2. ORTEP[33] drawing of 4 showing x-ray labelling scheme. Non-hydrogen atoms are drawn as principal ellipses at 50% probability level; H-atoms as small spheres of arbitrary size.

Structure Solution and Refinement. A unique octant was measured to $2\theta_{max} = 56°$ using an Enraf Nonius CAD-4 diffractometer in a θ-2θ scan mode with variable scan speeds (2.5 to 6.7 deg min^{-1}). A total of 3595 reflections were measured ($0 \le h \le 10$; $0 \le h \le 11$; $0 \le l \le 47$). Of these 2481 with $I \ge 3\sigma$ (I) were considered observed and used in full matrix least-squares refinement (on F) where the function minimized was $\Sigma w(|Fo-Fc|)$.[2] Structure solution was begun from a fragment located by direct methods and further elaborated by difference Fourier synthesis. Non-hydrogen atoms were refined with anisotropic thermal parameters. Positions for most of the hydrogen atoms were located from difference Fourier maps; those attached to carbon were held fixed at calculated positions along with fixed isotropic temperature factors 1.3 x U_C. Some of the hydrogens attached to water oxygens were not located. Residuals (on $|F|$) converged (max $\Delta/\sigma = 0.01$) to R=0.0468, R_w=0.0641 with the weights, w, defined as $1/s(Fo)^2$ with $s(Fo)^2=[\sigma(I)^2 + (0.05Fo)^2]^{1/2}$. An absorption correction was applied using the method of Walker & Stuart.[35] The goodness of fit was 1.78 based on a refinement with 367 variables. Occupancies of two of the water oxygens refined to 0.75 (03W) and 0.43 (04W). Neutral atom scattering factors[36] were used in computations with the SDP program system.[37] Maximum excursions in a final difference map were $\pm 0.292 eÅ^{-3}$. The atomic coordinates and interatomic distances and angles are found in Tables 3 and 4, respectively.

Bond distance arguments establish the predominate tautomeric keto form of the B ring in the solid state. For example, the C7-07 bond distance of 1.261(1)Å is within the range expected for aromatic carbonyls. Similarly, the N1-C2 distance of 1.343(4)Å is in the double bond range. Bond distances and angles in the remainder of the molecule compare favorably with values determined for camptothecin.[2] The A and B rings are rigorously planar. Rings C adopts an envelope while ring D adopts a twist-boat conformation. The E-ring conformation is a distorted half-chair. There is an extensive network of intermolecular hydrogen bonding interactions which stabilize the crystal lattice. Water oxygen 01 appears particularly tightly bound, forming interactions with both N1 and 07. Additional metrical details may be found in the deposited material which compromises structure factor amplitudes, thermal parameters, torsion angles and hydrogen-parameters.[38]

Table 3. Table of Positional Parameters and Their Estimated Standard Deviations

Atom	x	y	z	B(Å^2)*
01	0.1876(4)	0.6792(3)	0.47502(8)	3.60(6)
02	0 6566(6)	0.2803(7)	0.3701(1)	10.0(1)
03	0.5935(8)	0.5746(6)	0.1998(1)	7.3(1)
04	0.734(1)	0.473(1)	0.2173(2)	6.5(2)
07	0.3676(4)	-0.0595(3)	0.50185(7)	3.36(5)
017	0.4015(4)	0.2510(3)	0.63918(7)	3.44(6)
019	0.3409(3)	0.7055(3)	0.66532(6)	3.00(5)
020	0.5757(3)	0.8219(3)	0.64073(6)	2.60(5)
025	0.8923(4)	0.7054(3)	0.66199(7)	3.55(6)
026	1.0798(3)	0.9062(4)	0.70895(9)	4.66(7)
027	0.8812(5)	1.0770(5)	0.76013(8)	6.72(9)
029	0.5935(4)	1.2873(3)	0.70535(8)	4.55(7)
030	0.5838(3)	0.9901(3)	0.68723(6)	2.78(5)
N1	0.2967(4)	0.3866(3)	0.48389(8)	2.44(5)
N4	0.3478(4)	0.3135(3)	0.58012(8)	2.67(6)
C2	0.3089(4)	0.3313(4)	0.51821(9)	2.17(6)
C3	0.3016(4)	0.4237(4)	0.55215(9)	2.01(6)
C5	0.3454(6)	0.1593(4)	0.5663(1)	2.97(7)
C6	0.3339(5)	0.1842(4)	0.52541(9)	2.40(6)
C7	0.3481(4)	0.0781(4)	0.4968(1)	2.45(7)
C8	0.3358(4)	0.1412(4)	0.45952(9)	2.39(6)
C9	0.3507(5)	0.0506(4)	0.4280(1)	3.02(7)
C10	0.3382(6)	0.1083(5)	0.3933(1)	3.76(9)
C11	0.3107(7)	0.2602(5)	0.3882(1)	4.2(1)
C12	0.2963(6)	0.3524(4)	0.4183(1)	3.41(8)
C13	0.3110(5)	0.2939(4)	0.45385(9)	2.39(6)
C14	0.4210(4)	0.5550(4)	0.55296(9)	2.08(6)
C15	0.4449(4)	0.6164(4)	0.59206(9)	1.88(6)
C16	0.3935(4)	0.5099(4)	0.62238(9)	2.24(6)
C17	0.3827(5)	0.3492(4)	0.61504(9)	2.57(7)
C18	0.3491(5)	0.5593(4)	0.65551(9)	2.77(7)
C20	0.4011(5)	0.8119(4)	0.6389(1)	2.50(7)
C21	0.3568(5)	0.7663(4)	0.59957(9)	2.26(6)
C22	0.1686(5)	0.7595(4)	0.5945(1)	2.82(7)
C23	0.0861(5)	0.8214(5)	0.5674(1)	3.59(8)
C24	0.6413(5)	0.8475(4)	0.67600(9)	2.38(7)
C25	0.8306(5)	0.8459(4)	0.67370(9)	2.44(7)
C26	0.9031(5)	0.8903(5)	0.7110(1)	2.86(7)
C27	0.8292(5)	1.0364(5)	0.7242(1)	3.42(8)
C28	0.6376(5)	1.0292(4)	0.72359(9)	3.61(7)
C29	0.5566(6)	1.1757(5)	0.7323(1)	3.70(9)

*$B_{eq} = 4/3 \sum_i \sum_j B_{ij}\, a_i \cdot a_j$

Table 4. Principal Bond Distances(Å) and Angles(°)

Atoms	Distance	Atoms	Distance
O7-C7	1.261(3)	C6-C7	1.413(4)
O17-C17	1.252(4)	C7-C8	1.470(5)
O19-C18	1.365(4)	C8-C9	1.407(4)
O19-C20	1.436(4)	C8-C13	1.402(4)
O20-C21	1.401(4)	C9-C10	1.366(5)
O20-C24	1.400(4)	C10-C11	1.397(6)
O25-C25	1.421(4)	C11-C12	1.377(5)
O26-C26	1.420(4)	C12-C13	1.395(5)
O27-C27	1.413(4)	C14-C15	1.533(4)
O29-C29	1.433(5)	C15-C16	1.515(4)
O30-C24	1.422(4)	C15-C21	1.545(4)
O30-C28	1.430(3)	C16-C17	1.472(4)
N1-C2	1.343(4)	C16-C18	1.328(4)
N1-C13	1.377(4)	C20-C21	1.526(4)
N4-C3	1.465(4)	C21-C22	1.515(5)
N4-C5	1.475(4)	C22-C23	1.310(5)
N-C17	1.335(4)	C24-C25	1.513(5)
C2-C3	1.486(4)	C25-C26	1.523(4)
C2-C6	1.363(4)	C26-C27	1.519(5)
C3-C14	1.518(4)	C27-C28	1.531(5)
C5-C6	1.502(5)	C28-C29	1.502(5)

Atoms	Angle	Atoms	Angle
C18-O19-C20	116.9(3)	C14-C15-C21	107.5(2)
C20-O20-C24	115.1(2)	C15-C16-C17	120.4(2)
C24-O30-C28	112.8(2)	C15-C16-C17	120.4(2)
C2-N1-C13	120.1(3)	C17-C16-C18	118.4(3)
C3-N4-C5	113.5(2)	O17-C17-N4	121.2(3)
C3-N4-C17	123.1(3)	O17-C17-C16	124.0(3)
C5-N4-C17	123.4(3)	N4-C17-C16	114.8(3)
N1-C2-C3	123.8(3)	O19-C18-C16	124.8(3)
N1-C2-C6	123.2(3)	O19-C20-O20	110.2(3)
C3-C2-C6	113.0(3)	O19-C20-C21	111.5(3)
N4-C3-C2	100.6(2)	O20-C20-C21	106.9(3)
N4-C3-C14	110.8(2)	C15-C21-C20	107.1(3)
C2-C3-C14	115.3(2)	C15-C21-C22	113.3(3)
N4-C5-C6	101.3(2)	C20-C21-C22	110.7(3)
C2-C6-C5	110.0(3)	C21-C22-C23	124.9(4)
C2-C6-C7	121.8(3)	O20-C24-O30	106.8(2)
C5-C6-C7	128.1(3)	O20-C24-C25	108.7(3)
O7-C7-C6	124.6(3)	O30-C24-C25	110.3(3)
O7-C7-C8	121.3(3)	O25-C25-C24	111.8(3)
C6-C7-C8	114.1(3)	O25-C25-C26	111.5(3)
C7-C8-C9	121.1(3)	C24-C25-C26	109.2(3)
C7-C8-C13	121.5(3)	O26-C26-C25	111.0(3)
C9-C8-C13	117.4(3)	O26-C26-C27	108.4(3)
C8-C9-C10	121.4(3)	C25-C26-C27	111.1(3)
C9-C10-C11	120.4(3)	O27-C27-C26	113.6(3)
C10-C11-C12	119.8(4)	O27-C27-C28	108.6(3)
C11-C12-C13	119.9(3)	C26-C27-C28	110.3(3)
N1-C13-C8	119.3(8)	O3O-C28-C27	109.0(3)
N1-C13-C12	119.6(3)	O30-C28-C29	106.3(3)
C8-C13-C12	121.1(3)	C27-C28-C29	112.9(3)
C3-C14-C15	112.1(3)	O29-C29-C28	112.5(3)
C14-C15-C16	114.1(2)		

EXPERIMENTAL

General Methods: Melting points were obtained on a Thomas-Hoover melting point apparatus and are uncorrected. Optical rotations were performed in MeOH relative to the D line of sodium using a Jasco DIP-360 digital polarimeter equipped with a constant temperature bath held at 20°C. Infrared spectra were recorded on a Nicolet Model 20 DXB FTIR Spectrometer. Ultraviolet spectra were recorded on a Beckman DU-7 spectrophotometer. ^{1}H and ^{13}C-NMR spectra were obtained using a Bruker WM360 operating at ambient temperature (29°C) and included ^{1}H COSY and H/C correlation 2D NMR measurements, proton decouplings, ^{1}H J-resolved spectroscopy and ^{13}C edited spectra. All chemical shifts are reported with respect to TMS (δ0). Fast atom bombardment (FAB) mass spectra were obtained on a VG ZAB-HF mass spectrometer; the sample (ca. 10 μg) was dispersed on a stainless steel probe tip in a matrix of thioglycerol. FAB accurate mass measurements were made at an instrument resolution of 10,000 (M/ΔM) by linear voltage scanning using glycerol as the reference. NH_3-desorptive chemical ionization (DCI) mass spectra were obtained on a Finnigan MAT 4610 mass spectrometer using ca. 1 μg of sample. All solvents used were either HPLC or spectrophotometric grade.

Isolation of Alkaloids: Sample FB-12100B was received from Polysciences, Inc. (Warrington, PA, USA) as an opaque black viscous liquid containing suspended solids. This was the concentrate from the final one-third of the eluate from a large scale Amberlyst 15 column using 0.25% ammonia in isopropanol as the eluant. The starting material for this column was a portion of an isopropanol extract of sawdust from 24,000 pounds of *Camptotheca acuminata* logs. The IPA extractions were performed by Madis Laboratories (Hackensack, New Jersey, USA) using trees obtained from the USDA Plant Introduction Center (Chico, California, USA).

Sample FB-12100B was partitioned between water and ethyl acetate. The organic layer was concentrated to dryness and was triturated with diethyl ether and the solution filtered to give 45 grams of precipitate which was chromatographed on silica gel (EM Reagents Silica Gel 60, 70-230 mesh, 2 kg) using increasing amounts of methanol in methylene chloride to give samples of crude camptothecin (**1**), 10-hydroxycamptothecin (**2b**), 18-hydroxycamptothecin (**2e**) and angustoline (**3**). Compounds **1**, **2b**, **2e** and **3** were further purified by crystallization from CH_2Cl_2/MeOH and their structures were determined by comparison of their spectral data with published values.

The aqueous portion of sample FB-12100B was extracted with n-butanol and the butanol layer was evaporated *in vacuo* to give 118 grams of solids which were triturated with 1/1 MeOH/CH_2Cl_2. The MeOH/CH_2Cl_2 solubles were chromatographed repeatedly on Sephadex LH-20 (500 grams) to give a crude glycoside which was crystallized from aqueous methanol after slow evaporation at elevated temperature (40°C) to give pure **4**.

Glycoside (**4**): mp 288-290°C (1/1 MeOH/H_2O); $[\alpha]^{20}$ - 138.8° (C=0.5, MeOH); IR (KBr) 3600-3100, 3100-3000, 3000-2800, 1652, 1633, 1611, 1595, 1582, 1561, 1513 cm^{-1}; UV (CH_3CN) 240 nm (ε 39,500), 315 nm (ε 10,200), 328 nm (ε 11,800); UV (CH_3CN + HCl) 235 nm (ε 5900), 310 nm (ε 8900), ^{1}H and ^{13}C NMR - Table 1; high resolution FABMS found m/z 513.1870, $C_{26}H_{29}N_2O_9$ (M + H) requires m/z 513.1873.

Acid Hydrolysis of Glycoside 4: A sample of the glycoside 4 (70 mg) was heated at reflux with 2M methanolic HCl for 5 h. The reaction mixture was cooled and the HCl was removed under a stream of nitrogen. The resulting residue was partitioned between water and CH_2Cl_2. The aqueous layer was evaporated and chromatographed on reversed-phase HPLC (Dynamax C18, 25% CH_3CN/H_2O) to give the aglycone 6. IR (KBr) 3449, 1654, 1637, 1587, 1169, 1093 cm^{-1}; ^1H NMR [$(CD_3)_2SO$] δ 1.37 (q, 1H, J = 12.3 Hz), 2.49 (m, 1H), 2.75 (m, 1H), 3.00 (m, 1H), 3.46 (s, 3H), 4.25 (d, 1H, J = 14.7 Hz), 4.72 (d, 1H, J = 14.7 Hz), 4.97 (s, 1H), 5.18 (bd, 1H, J = 10 Hz), 5.30 (d, 2H, J = 17.2 Hz), 5.42 (m, 1H), 7.33 (t, 1H, J = Hz), 7.37 (bs, 1H), 7.60 (t, 1H, J = 8 Hz), 7.64 (d, 1H, J = 8 Hz), 8.12 (d, 1H, J = 8 Hz). ^{13}C NMR [$(CD_3)_2SO$] δ 176.0 (s), 161.6 (s), 148.5 (s), 146.7 (d), 140.5 (s), 132.7 (d), 131.4 (d), 125.2 (s), 124.7 (d), 123.1 (d), 119.8 (t), 118.0 (d), 112.8 (s), 106.9 (s), 101.0 (d), 60.3 (d), 55.5 (q), 48.1 (t), 42.6 (d), 29.0 (t), 28.0 (d); low resolution DCI MS found m/z 365 for $C_{21}H_{21}N_2O_4$ (M + H).

Acknowledgment. The authors would like to thank Dr. Randall Johnson of SmithKline Beecham, Dr. Homer Sims of Polysciences, Inc., Warrington, PA and Dr. Matthew Suffness of the NCI for providing the extracts of *Camptotheca acuminata* used in this study.

REFERENCES

1. Wall, M. E.; Wani, M. C.; Cook, C. E.; Palmer, K. H.; McPhail, A. T.; Sim, G. A. *J. Am. Chem. Soc.* **1966**, *88*, 3888.
2. McPhail, A. T.; Sim, G. A. *J. Chem. Soc., B*, **1968**, 923.
3. Govindachari, T. R.; Viswanathan, N. *Indian J. Chem.* **1972**, *10*, 453.
4. Tafur, S.; Nelson, J. D.; DeLong, D. C.; Svoboda, G. H. *Lloydia* **1976**, *39*, 261.
5. Gunsekera, S. P.; Badaw, M. M.; Cordell, G. A.; Farnsworth, N. R.; Chitnis, M. *J. Nat. Prod.* **1979**, 42, 475.
6. Hutchinson, C. R. *Tetrahedron* **1981**, *37*, 1047.
7. Hsiang, Y. H.; Hertzberg, R.; Hecht, S.; Liu, L. F. *J. Biol. Chem.* **1985**, *260*, 14873.
8. Stewart, A. F.; Shutz, G. *Cell* **1987**, *25*, 1109.
9. Thomsen, B.; Mollerup, S.; Bonwen, B. J.; Frank, R.; Blocker, H.; Nelson, O. F.; Westergaard, O. *EMBO J.* **1987**, *6*, 1817.
10. Mattern, M. R.; Mong, S. M.; Bartus, H. F.; Mirabelli, C. K.; Crooke, S. T. *Cancer Res.* **1987**, *47*, 1793.
11. Govindachari, T. R.; Viswanathan, N. *Phytochemistry* **1972**, *11*, 3529.
12. Agarwal, J. S.; Rastogi, R. P. *Indian J. Chem.* **1973**, *11*, 969.
13. Wani, M. C. Wall, M. E. *J. Org. Chem.* **1969**, *34*, 1364.
14. Lin, L. T.; Sung, C. C.; Hsu, J. S. *K'o Hseuh Tung Pao* **1979**, *24*, 478; *Chem. Abs.* **1979**, *91*, 193482u.

15. Lin, L. Z.; Zhang, J. S.; Shen, J. H.; Zhou, T.; Zhang, W. Y. *Acta Pharmaceutica Sinica* **1988**, *23*(3), 186.

16. Kingsbury, W. D.; Hertzberg, R. P.; Boehm, J. C.; Holden, K. G.; Jakas, D. R.; Caranfa, M. J.; McCabe, F. L.; Faucette, L. F.; Johnson, R. J. *Proc. Amer. Assoc. Cancer Res* **1989**, *30*, 622.

17. a) Au, T. Y.; Cheung, H. T.; Sternhell, S. *J. Chem. Soc. Perkin I* **1973**, 13. b) Phillipson, J. D.; Hemingway, S. R.; Bisset, N. G.; Houghton, P. J.; Shellard, E. J. *Phytochemistry* **1974**, *13*, 973.

18. Aimi, N.; Nishimura, M.; Hoshino, H.; Sakai, S.; Haginiwa, J. *Tetrahedron Letters* **1989**, *30*, 4991.

19. Poehland, B. L.; Troupe, N.; Carte', B. K.; Westley, J. W. *J. Chromatography* **1989**, *481*, 421.

20. Bock, K.; Lundt, I.; Pederson, C. *Tetrahedron Letters* 1973, 1037.

21. Brown, N. M. D.; Grundon, M. F.; Harrison, D. M.; Surgenor, S. A. *Tetrahedron* **1980**, *36*, 3579.

22. Haasnoot, C. A. G.; DeLeeuw, F. A. A. B.; Altona, C. *Tetrahedron* **1980**, 2783.

23. Barfield, M.; Sternhell, S. *J. Am. Chem Soc.* **1972**, *94*(6), 1903.

24. Wenkert, E.; Dave, K. G.; Lewis, R.G.; Sprague, P. W. *J. Am. Chem. Soc.* **1967**, *89*, 6741.

25. Winterfeldt, E. *Liebigs Ann. Chem.* **1971**, *745*, 23

26. Hutchinson, C. R.; Heckendorf, A. M.; Daddona, P. E.; Hagman, E.; Wenkert, E. *J. Am. Chem. Soc.* **1974**, *96*, 5609.

27. Battersby, A. R.; Burnett, A.R.; Parsons, P. G. *J. Chem. Soc. C* **1969**, 1193.

28. Hutchinson, C. R.; Heckendorf, A. M.; Straughn, J. L.; Daddona, P. E.; Cane, D. E. *J. Am. Chem. Soc.* **1979**, *101*, 3358.

29. Cordell, G. A. *Lloydia* **1974**, *37*, 219.

30. Dolby, L. J.; Booth, D. L. *J. Am. Chem. Soc.* **1966**, *88*, 1049.

31. Witkop, B.; Patrick, J. B. *J. Am. Chem. Soc.* **1951**, *73*, 2196.

32. Witkop, B.; Goodwin, S. *J. Am. Chem. Soc.* **1953**, *75*, 3371.

33. Johnson, C. K. *ORTEP II*. Report ORNL-5138. Oak Ridge National Laboratory, Tennessee, USA **1976**.

34. Asher, J. D. M.; Robertson, J. M.; Sim, G. A.; Bartlett, M. F.; Sklar, R.; Tayler, W. I. *Proc. Chem. Soc.* **1962**, *72*, 6354.

35. Walker, N.; Stuart, D. *Acta Cryst.* **1983**, *A39*, 158.

36. International Tables for X-ray Crystallography, Vol. IV. Birmingham: Kynoch Press **1974** (Present Distributor Kluwer Academic Publishers, Dordrecht).

37. Frenz, B. A. Enraf-Nonius Structure Determination Package **1987**, Enraf-Nonius, Delft, The Netherlands.

38. Supplementary data available. See notice to Authors, *Tetrahedron* **40**(2) ii (1984).